Available online at www.sciencedirect.com
ScienceDirect
Tectonophysics 442 (2007) 66–82
TECTONOPHYSICS
www.elsevier.com/locate/tecto

A deterministic seismic hazard analysis for shallow earthquakes in Greece

L. Moratto [a,*], B. Orlecka-Sikora [b], G. Costa [a], P. Suhadolc [a], Ch. Papaioannou [c], C.B. Papazachos [d]

[a] *Department of the Earth Sciences, University of Trieste, Italy*
[b] *Department of Geophysics, Faculty of Geology, Geophysics and Environmental Protection, AGH University of Science and Technology, Krakow, Poland*
[c] *ITSAK, Thessaloniki, Greece*
[d] *Department of Geophysics, Aristotle University of Thessaloniki, Greece*

Received 23 June 2006; received in revised form 27 April 2007; accepted 8 May 2007
Available online 7 June 2007

Abstract

The maximum expected ground motion in Greece is estimated for shallow earthquakes using a deterministic seismic hazard analysis (DSHA). In order to accomplish this analysis the input data include an homogeneous catalogue of earthquakes for the period 426 BC–2003, a seismogenic source model with representative focal mechanisms and a set of velocity models. Because of the discrete character of the earthquake catalogue and of errors in location of single seismic events, a smoothing algorithm is applied to the catalogue of the main shocks to get a spatially smoothed distribution of magnitude. Based on the selected input parameters synthetic seismograms for an upper frequency content of 1 Hz are computed on a grid of $0.2° \times 0.2°$. The resultant horizontal components for displacement, velocity, acceleration and DGA (Design Ground Acceleration) are mapped. The maps which depict these results cannot be compared with previously published maps based on probabilistic methodologies as the latter were compiled for a mean return period of 476 years. Therefore, in order to validate our deterministic analysis, the final results are compared with PGA estimated from the maximum observed macroseismic intensity in Greece during the period 426 BC–2003.

Since the results are obtained for point sources, with the frequency content scaled with moment magnitude, some sensitivity tests are performed to assess the influence of the finite extent of fault related to large events. Sensitivity tests are also performed to investigate the changes in the peak ground motion quantities when varying the crustal velocity models in some seismogenic areas. The ratios and the relative differences between the results obtained using different models are mapped and their mean value computed. The results highlight the importance in the deterministic approach of using good and reliable velocity models.

Keywords: Seismic hazard; Greece; Deterministic model; Velocity models

1. Introduction

Seismic hazard analysis is among the most common tool to estimate the expected level of intensity of ground motion which is related to seismic events, so it is the fundamental input into the decision-making process for

* Corresponding author. Tel.: +39 040 558 2121.
E-mail address: morattol@dst.units.it (L. Moratto).

0040-1951/$ - see front matter © 2007 Elsevier B.V. All rights reserved.
doi:10.1016/j.tecto.2007.05.004

earthquake loss mitigation (McGuire, 1993). There are two possible approaches for estimating the seismic hazard: the deterministic (DSHA) and the probabilistic (PSHA) seismic hazard analysis. These two methods can complement each other, thus providing additional insights into the question of seismic hazard.

Even though several seismic hazard maps were compiled for Greece since the 1970s using as seismic hazard parameter either the macroseismic intensity (Papaioannou, 1984; Papazachos et al., 1985; Papaioannou, 1986; Papaioannou and Papazachos, 2000), or the peak ground acceleration and velocity (Algermissen et al., 1976; Drakopoulos and Makropoulos, 1983; Papazachos et al., 1990, 1993; Margaris, 1994; Koutrakis et al., 2002; Burton et al., 2002), most of them correspond to mean return periods of 476 or 975 years. However, the design of critical infrastructures demands even longer return periods. Therefore, the knowledge of the distribution of the maximum ground values based on reliable methodologies is still a critical issue.

The aim of the present study is to compile maps illustrating the geographical distribution of the upper bound of ground motion values for the area of Greece using the most recent seismological data through a reliable DSHA methodology already applied in several regions of Euro Mediterranean area (Costa et al., 1993; Orozova-Stanishkova et al., 1996; Aoudia et al., 2000; Bus et al., 2000; Markusic et al., 2000; Radulian et al., 2000; Zivcic et al., 2000; El-Sayed et al., 2001). Deterministic procedures use available seismicity catalogues, geological and velocity model data and the known seismic source parameters near the investigated site to generate models of ground motion at that site. Usually one or more earthquakes are specified by their magnitude and location with respect to the site. The magnitude, source parameters, source-to-site distance with a given velocity model, along with site conditions, are all input parameters for the deterministic calculations through synthetic seismograms of the maximum possible site ground motion. This is also our approach (Costa et al., 1993) in which the synthetics are computed with the modal summation technique (Panza, 1985; Panza and Suhadolc, 1987; Florsch et al., 1991). The results of this approach are the maps of the resultant peak horizontal ground motion distribution (displacement, velocity, acceleration and design ground acceleration) over the investigated territory. This method allows the evaluation of the contribution of each parameter on the final result. The maps which depict these results cannot be compared with previously published maps based on probabilistic methodologies as the latter were compiled for a mean return period of 476 years. Therefore, in order to validate our deterministic analysis, the final results are compared with PGA estimated from the maximum observed macroseismic intensity in Greece during the period 426 BC–2003.

Another important aim of this paper is to perform some sensitivity tests. The first one to assess the range of peak ground motion quantities obtained when different crustal velocity models, proposed for a given seismogenic area, are used in the calculations. We demonstrate that the strongest differences are due to changes in the velocities of the near surface layers.

Since all results are obtained for point source, with the frequency content scaled with moment magnitude, some sensitivity tests are performed to assess the influence of the finite extent of fault related to large events on the final results. We compare PGV values related to the Kozani on May 13, 1995 earthquake computed with a finite source model (Suhadolc et al., 2007), with those obtained from our deterministic approach based on point sources. The results show that the strongest differences on the final results are mainly due to the directivity effect but, on the other side, the application of a smoothing window reduces the influence of the source spatial extent.

2. Tectonic setting and seismicity of the area of Greece

The Aegean and surrounding areas lay on the most active part of the Africa–Eurasia collision zone, which is responsible for the very high level of seismic activity in this region. More than 60% of the European seismicity is expected to occur in this region with earthquake magnitudes up to $M_w = 8.2$ (Papazachos, 1990). This is related to the compressional motion between Europe and Africa (Fig. 1), giving rise to the subduction of the eastern Mediterranean lithosphere, the front part of the African lithosphere, under the Aegean along the Hellenic Arc (Papazachos and Comninakis, 1969), and the westward motion of the Anatolian block along the North Anatolia Fault (McKenzie, 1970). The Aegean has been recognized to form a separate Aegean microplate moving towards the southwest with respect to Eurasia (McKenzie, 1972; Jackson, 1994; Papazachos et al., 1998; Papazachos, 1999). The tectonic processes that occur in the subducting slab in the Aegean area control the distribution of both seismicity and volcanism (Karagianni et al., 2002, 2005).

The shallow seismicity occurring along the whole Aegean back-arc area is mainly associated with normal faults (McKenzie, 1978). Dextral strike-slip faults are observed in northern Turkey, like the North Anatolian fault and its continuation along both the North Aegean

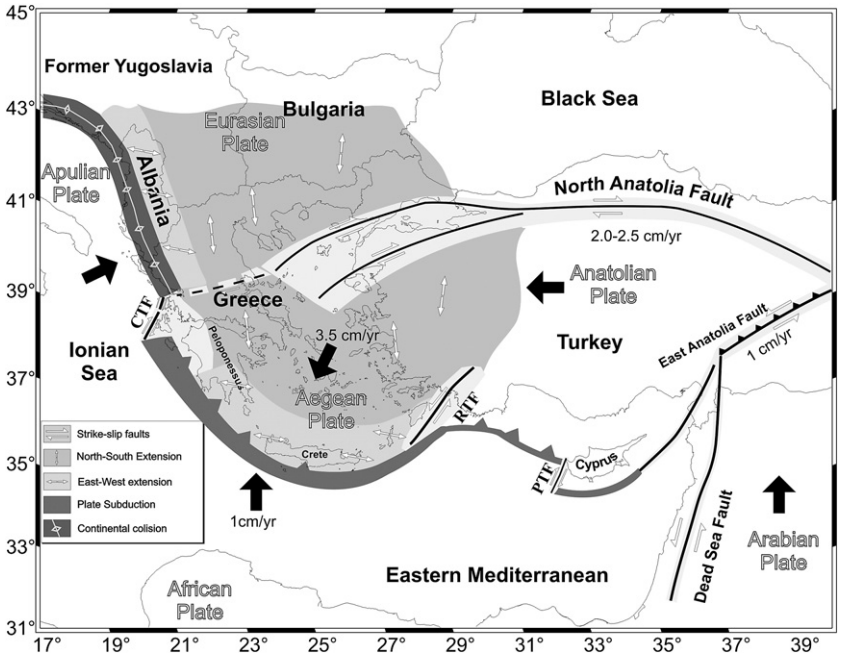

Fig. 1. Tectonic features in Greece modified from Papazachos et al. (1998).

Trough and the Cephalonia Fault (Scordilis et al., 1985). Dextral strike-slip faults are also observed in the Aegean, especially in the South Aegean Trough (Taymaz et al., 1991). An intense shallow seismicity with low-angle thrust faults appears along the Hellenic arc (Papazachos, 1990). The exterior part of the Hellenic arc forms the sedimentary arc, whereas the interior part is a volcanic arc. The Hellenic trench bounds the outer borders of the Hellenic arc.

3. Seismogenic zones

One of the first steps of our seismic hazard analysis is to identify seismogenic zones, which are seismotectonically homogeneous areas. Using various seismological criteria (e.g. maximum magnitude, seismicity rate, rate of moment release) these zones are divided into smaller subzones called seismic sources. Each of the selected seismic sources is also characterized by a representative focal mechanism. This procedure reduces the amount of computations. As already mentioned, the DSHA algorithm we use enables us to analyze different models of seismogenic zonations, different seismic source parameters and different structural velocity models. Available recent studies on the seismic zonation in the Aegean and surrounding areas (Papaioannou and Papazachos, 2000) have been used to separate the Aegean and surrounding areas into 67 seismogenic sources of shallow earthquakes; at the same time seven seismogenic sources have been defined for intermediate-depth earthquakes in the Southern Aegean (Papazachos and Papaioannou, 1993; Papaioannou and Papazachos, 2000). In this study only the 67 seismogenic zones for shallow earthquakes are used (Fig. 2) to assess the seismic hazard.

4. Representative fault plane solutions

One of the input parameters needed to compute synthetic seismograms is the earthquake mechanism.

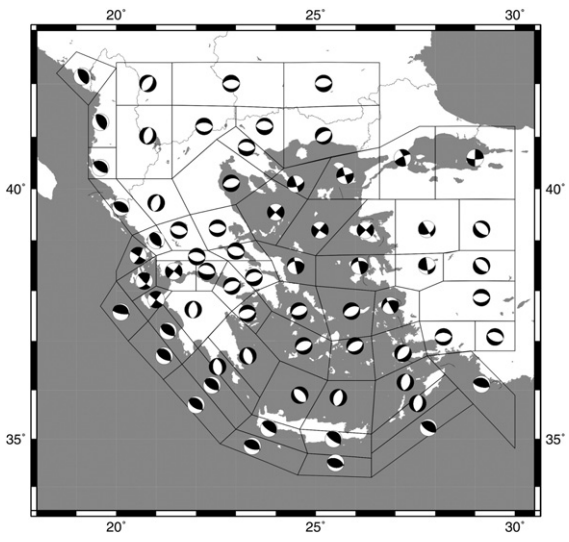

Fig. 2. The fault plane solutions assigned to every seismogenic source.

Table 1
Focal mechanisms (strike, dip and rake) selected for the 67 seismogenic zones used in the DSHA

Area	Name	Strike	Dip	Rake
1	Montenegro	325	29	85
2	Dyrarachium	334	27	93
3	Avlona	309	27	93
4	Igoumenitsa	300	43	90
5	Preveza	340	43	113
6	Leukada	30	77	178
7	Cephalonia	40	57	172
8	Zante	37	89	176
9	Pylos	320	32	106
10	Mane	320	32	106
11	Ionian Sea-1	310	18	118
12	Ionian Sea-2	320	32	106
13	Ionian Sea-3	320	32	106
14	SW Crete	315	17	99
15	SE Crete	315	17	99
16	Libyan Sea-1	305	29	105
17	Libyan Sea-2	291	47	99
18	Karpathos	184	47	262
19	Strabo	303	25	90
20	Marmaris	294	27	99
21	Piskope	30	49	263
22	Ochrida	189	49	263
23	Drosopighe	11	49	263
24	Tripolis	358	47	262
25	Cythera	346	47	262
26	Leonidi	340	47	262
27	NW Crete	313	47	262
28	NE Crete	10	47	262
29	Rhodos	185	47	262
30	Philipoupolis	270	37	276
31	Kresna	266	53	267
32	Drama	62	37	272
33	Serres	90	53	267
34	Ptolemais	270	53	267
35	Volvi	93	53	267
36	Kozani	253	43	265
37	Thessalia	271	47	272
38	Cremasta	283	47	272
39	Agrinio	281	47	272
40	Maliakos	282	47	270
41	Thebes	256	40	270
42	Patra	37	89	184
43	Aeghio	290	30	281
44	Corinth	253	44	276
45	Methana	266	48	282
46	Melos	250	45	270
47	Thera	65	40	270
48	Cos	50	48	282
49	Alikarnassos	80	42	261
50	Denisli	280	42	261
51	S. Euboikos	80	48	282
52	Ikaria	65	40	270
53	Samos	244	45	245
54	Aydin	83	42	261
55	Kyme	261	45	205
56	Chios	261	45	205
57	Izmir	83	45	245
58	Alashehir	313	34	270
59	Skiathos	225	89	188
60	Skyros	216	86	185
61	Lesbos	45	89	188
62	Demirci	61	45	245
63	Gediz	312	35	270
64	Athos	72	64	183
65	Samothrace	253	88	190
66	Hellispontos	245	80	165
67	Brussa	91	76	179

Papazachos et al. (2001) estimated the main parameters of the 159 faults of major shallow earthquakes, which have occurred since 480 BC in the broader Aegean area. On the basis of faulting type and fault orientation, fault plane solutions have been divided into ten groups. The first and third groups are distributed along the Hellenic Arc and their continuation, North of the Cephalonia fault, along the western coast of northern Greece, Albania and Montenegro. They represent thrust faults connected with the subduction of the eastern Mediterranean beneath the Aegean and the collision of the Adriatic microplate with the western Greek-Albanian coast. The second group includes strike-slip faults along the Cephalonia fault, whereas the tenth group represents strike-slip faulting along the North Aegean Trough. The fourth and fifth groups of faults are N–S orientated normal faults connected with the subduction–collision tectonics of the thrust-fault zone of the Hellenic Arc. The other groups extend from southern Aegean up to southern Bulgaria and are dominated by normal faults trending E–W on the average (Papazachos, 2002). Papazachos et al. (1999a) defined the rupture zones for 150 strong shallow earthquakes in the Aegean region and determined the type of faulting. The representative focal mechanisms for every seismogenic zone were selected (Table 1) using those proposed by Papazachos and Papazachou (2003) and their geographical distribution is shown in Fig. 2.

5. Earthquake catalogue

In order to estimate the maximum ground motion in the area of Greece the seismicity catalogue of the Geophysical Laboratory of the Aristoteles University in Thessaloniki (http://lemnos.geo.auth.gr/the_seisnet/WEBSITE_2005/CATALOGS/seiscat.dat) is used. The catalogue is homogeneous with respect to magnitude since all magnitudes are given in a scale equivalent to the moment magnitude. The catalogue includes earthquakes

in the period 426 BC–2003. The source parameters of the first part of the catalogue, which includes the historical earthquakes (426 BC–1899), are determined using the available macroseismic data and are based on the catalogue of Papazachos and Papazachou (2003) that includes earthquakes with $M \geq 6.0$. The magnitude errors for this period vary between ±0.35 and ±0.50 of the magnitude unit depending on the quantity of the available macroseismic information. For the historical earthquakes the epicenters have usually an error of about 30 km but this error can reach up to 50 km when the number of available macroseismic data is less than 5. The source parameters of the instrumental era (1900–2003) are based on the catalogue of Comninakis and Papazachos (1986) for the period 1900–1985. For the period 1986–2001 the ISC data are used, while for the last period the data come from the seismological network of the Aristoteles University at Thessaloniki. The errors in the magnitudes are in the interval ±0.25 for the instrumental period. The errors of the epicentral coordinates for the earthquakes of the period 1965–1999 vary between 10 and 20 km. The epicenter locations for the period 1901–1964 were calculated by both instrumental and macroseismic information and their errors can be up to 30 km. The completeness of this catalogue is shown in Table 2. Because in the deterministic approach one is essentially interested in the effects of the strongest events, the completeness of the catalogue plays a less crucial role than in PSHA. We can see that the catalogue is complete for damaging ($I_{MM} \geq$ VII) events in the last hundred years and for destructive ($I_{MM} \geq$ IX) events for the last five centuries. The spatial distribution for stronger events ($M > 5.0$) is reported in Fig. 3.

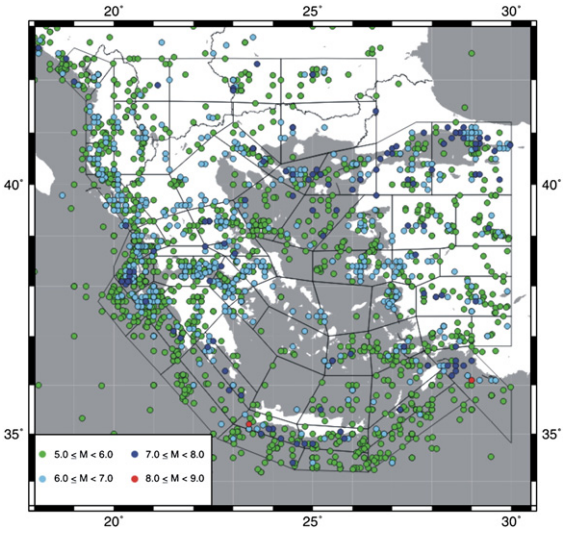

Fig. 3. Epicenters of earthquakes with $M_w \geq 5.0$ for the historical catalogue.

6. Velocity models

On the basis of the structural and geological characteristics, the investigated area is divided into eight structural polygons (Fig. 4). A flat, layered 1-D velocity model is associated with each polygon. The different layers are described by their thickness, density, P and S-wave velocities and attenuation (Papazachos, 2002). The models do not explicitly account for local site effects, and are therefore representative of regional average properties (bedrock) within each polygon.

The upper frequency of our computations is 1 Hz, therefore the structural models have to reach to a depth of about 1100 km to be able to compute synthetic seismograms with the modal summation technique (Panza,

Table 2
The completeness of the Greek seismic catalogue (Papazachos and Papazachou, 2003)

Period of catalogue completeness	Moment magnitude
426 BC–1500	$M \geq 8.0$
1501–1840	$M \geq 7.3$
1841–1900	$M \geq 6.5$
1901–1910	$M \geq 6.0$
1911–1949	$M \geq 5.2$
1950–1964	$M \geq 4.8$
1965–1980	$M \geq 4.5$
1981–2003	$M \geq 4.0$

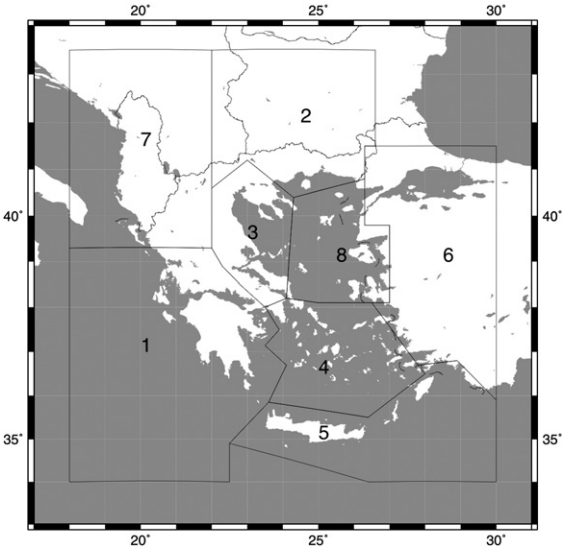

Fig. 4. Regional polygons associated with different lithospheric velocity models.

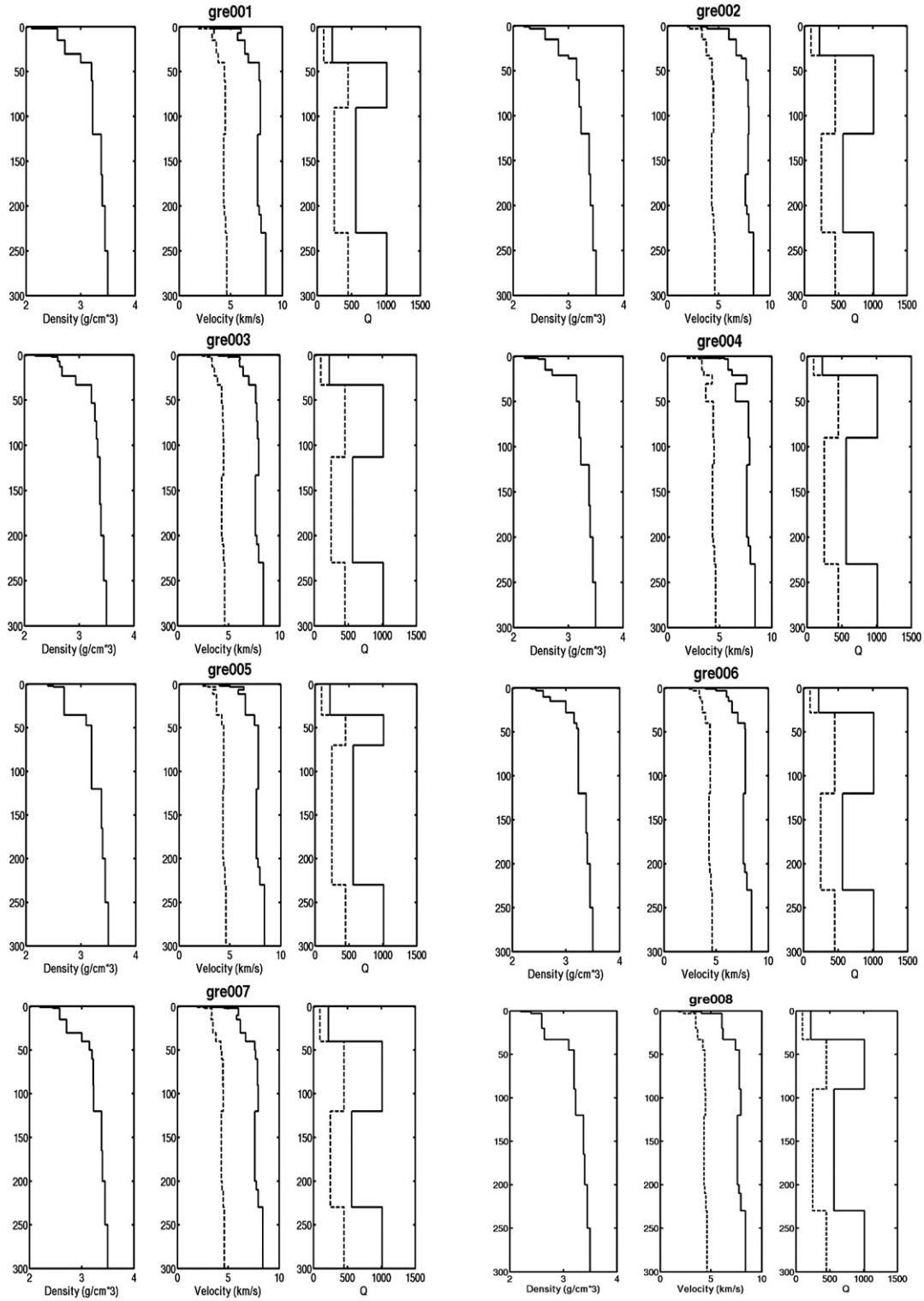

Fig. 5. Lithospheric velocity models as a function of depth (solid lines show P-wave data, dotted lines show S-wave data) for the polygons considered in this study.

1985; Panza and Suhadolc, 1987; Florsch et al., 1991). We have proposed specific crust–uppermost mantle models down to a depth of about 100 km and then the models have been completed adding for depths greater than 100 km the results proposed by Costa et al. (1993) for the Eastern Europe zone. To model the lithospheric structures in the different polygons we have selected the data proposed by Karagianni et al. (2002, 2005) who derived a 3-D tomographic image of the shear-wave velocity structure of the crust–uppermost mantle in the Aegean area inverting group velocities of the Rayleigh wave fundamental mode. After fixing the shear-wave velocity values, the P-wave velocities have been computed using the Poisson ratio, whereas the density values have been obtained from the Birch law and from the Nafe–Drake curves (Fowler, 1991). In case no velocity values were available the P-wave velocity at the surface has been fixed at 4 km/s. The Q values are relatively low in the crust (Q_α=225; Q_β=100), whereas under the Moho discontinuity they are higher (Q_α=1000; Q_β=450) and in the asthenospheric channel (Q_α=550; Q_β=200) (Lay and Wallace, 1995, p. 110) somewhere smaller.

As mentioned in the second section, the Aegean region is an area of complex tectonics at the convergence zone of the Eurasian and African lithospheric plates, and this fact is reflected in the complexity and strong variation of the structural models over the Aegean area. A thin crust approximately 20–30 km thick has been proposed for the central and southern Aegean sea, whereas a significant crustal thickness (40–47 km) has been identified along the Hellenides mountain range; the crust has an average thickness of 28–37 km in the eastern part of the Greek mainland, in the northern and central Aegean, in western Turkey and in Crete (Karagianni et al., 2002, 2005). Karagianni et al. (2005) have detected in the depth range from 5 to 20 km a low-velocity zone in western Greece under Peloponnesus and Rhodes (polygons 1 and 5). This low-velocity zone, observed also previously by Papazachos et al. (1995) and Papazachos and Nolet (1997), extends along the Hellenic arc and can be correlated with the Hellenides mountain range and the alpine orogenesis, in accordance with the ideas of weakening mid-crustal intrusions (Mueller, 1977). Low shear-wave velocities extend over the central and southern Aegean Sea (polygon 4) for depths ranging from 30 to 40 km (Karagianni et al., 2005). These velocities, which are found just below the Moho discontinuity, can be correlated with the high heat flow in the mantle wedge above the subducted slab and the related active volcanism in the area (Papazachos and Nolet, 1997). These values are usually attributed to the presence of partial melt in the mantle wedge and correspond to unusually high melt fractions of the order of 15–20% for a typical mantle composition (Birch, 1969). Our eight structural models are plotted in Fig. 5. All proposed models are in overall agreement with previous studies (Papazachos et al., 1995; Papazachos and Nolet, 1997; Novotny et al., 2001; Zahradnik and Papatsimpa, 2001; Karagianni et al., 2002, 2005). The eight structural models are used to compute the frequency-dependent quantities needed to generate synthetic seismograms.

7. Computation

A deterministic seismic hazard assessment (DSHA) approach to estimate the expected maximum level of ground acceleration has been developed by Costa et al. (1993). Ground motions at the sites of interest are evaluated using synthetic seismograms, which are computed on the basis of the knowledge of the seismic source physical processes and wave propagation in a realistic 1-D medium.

The investigated area is divided into cells with size $0.2° \times 0.2°$ chosen on the basis of experience and approximately equal to the standard error in earthquake epicenter determination (Suhadolc, 1990; Panza et al., 1990). Seismic sources are defined only in the cells located within a seismogenic source. A double-couple point source is placed in the center of each cell and for each seismogenic source a representative focal mechanism is selected. The sources and the receivers do not overlap, because the sources are placed in the center of each cell covering the entire investigated region whereas the receivers are placed at the cell corners (Costa et al., 1993). The distribution of the maximum magnitude over the investigated territory is needed to appropriately scale the computed synthetic seismograms. To obtain this distribution the seismicity of the shallow earthquakes catalogue is analyzed (the maximum earthquake depth considered is 50 km). Data available from earthquake catalogue are discrete and earthquake catalogues are incomplete and affected by errors, so a smoothed distribution is preferable (Panza et al., 1990). We smoothed our data separately for each seismogenetic zone to have a magnitude distribution in agreement with the criteria for selecting seismic sources zones. In cells with no data a default magnitude value (M=5.0) has been assigned because in each area of the seismogenic zone a medium size earthquake can occur.

The magnitude value of the strongest event that occurred within a cell has been assigned to the cell. The discretization does not warrant the statistically meaningful number of events in each cell, so the maximum magnitude to be associated with each cell has been

searched for also in the surrounding cells, through the application of a centered smoothing window (Costa et al., 1993). The maximum value of magnitude found in the window has been assigned to the central cell only if the cell itself contains a minimum number of earthquakes. For this purpose three possible smoothing windows have been selected. Their "radius" is expressed in terms of the number of cells, n. The values $n=1$, $n=2$, $n=3$ are considered and by applying those windows to the distribution, the results have been obtained. The smoothing algorithm has been applied separately for each seismogenetic area and the catalogue of strong shock for the Greece territory has been used. The geographical distribution of the results after the maximum magnitude value has been assigned at each cell, and the map in Fig. 6 depict the smoothed magnitude distribution for the cells belonging to the seismogenic sources; the window applied has a radius $n=3$.

The choice of the cell size and the procedure of the smoothing window were discussed extensively by Costa et al. (1993). As already mentioned, the dimension 0.2° of the cells can be related with errors in the location of earthquakes, even if for historical earthquakes such a resolution could be considered optimistic. The procedure requires a distribution over the territory of the maximum magnitude but earthquake catalogues are discrete, incomplete and affected by errors: the smoothed magnitude allow us to resolve these problems and to take into account the case of cells that do not contain a meaningful

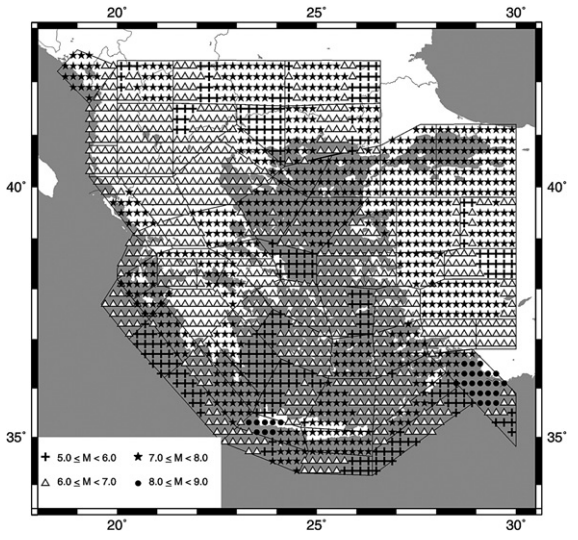

Fig. 6. Smoothed magnitude distribution after the application of discretization to the seismicity data ($M \geq 5.0$ and depth ≤ 50 km) of the Greece catalogue (Papazachos, 2002), the intersection between the seismogenic sources of Fig. 2 and the magnitude discretization. Radius of smoothing window $n=3$.

number of events. Costa et al. (1993) tested several thresholds for the minimum number of earthquakes of each cell to consider; only areas with a low seismicity level are sensitive to modification of this threshold but consideration of seismogenic zones ensures stability. Different radius for the smoothing window was tested for the Italian territory and a radius $n=3$ gives a good degree of homogeneity in the distribution of magnitude.

The procedure of synthetic seismograms computation enables us to perform detailed parametric analyses: different source parameters and structural models can be taken into account in order to evaluate a wide range of possible scenarios. At the beginning the synthetic seismograms have been computed for a low seismic moment of 10^{13} N·m obtaining a flat source spectrum and then a spectral scaling law (Gusev, 1983) has been applied to get the final amplitude results. If the source–receiver path crosses one or more boundaries, the seismograms have been computed using the receiver structural model, since we assume the final signals have been influenced more by the receiver structural model than by the source one. The program computes radial, transversal and vertical seismograms and the resultant of the horizontal components has been computed. The largest amplitude seismograms, due to any of the surrounding sources, has been selected and associated with each particular site. To reduce the number of the computed seismograms, we have limited the maximum distance between the source and the sites where the ground motions are calculated, so the maximum distance is a function of the source magnitude. The maximum distance is equal to 25 km for $M<6.0$, is equal to 50 km for $6.0<M<7.0$ and is equal to 90 km if $M>7.0$. The choice of the maximum epicentral distance for computing synthetic seismograms is supported by computation of ground motion parameters using the empirical relations of Ambraseys et al. (2005). Being the source placed in the center of the cell and the receiver at the edge, the epicentral distance must be larger than 14 km; the ground motion relations (Ambraseys et al., 2005) give us a PGA value of 0.035 g, associated approximately with a macroseismic intensity VI, for a seismic event with $M=5.0$ at a distance of 25 km. So even if at larger distances we can be strongly shaken by the event, the damage on buildings and civil structures are confined near the source. The empirical relations therefore validate our distance limitations imposed to reduce the computation time. A constant hypocentral depth of 10 km has been assigned to all sources.

Displacements, velocities and accelerations have been computed for an upper frequency of 1 Hz. For acceleration in particular, this upper frequency limit is rather low, but an estimate of the PGA can be obtained

by computing the design acceleration, DGA at zero period, scaling the EC8 normalized design response spectrum (normalized elastic acceleration spectra of the ground motion for 5% critical damping) with the response acceleration spectrum (Panza et al., 1996). The calculations are carried out for bedrock sites that are ground type A according to EC8.

8. Seismic hazard results

Using the previously described input data we performed a deterministic seismic hazard analysis (DSHA) for the broader area of Greece using the methodology proposed by Costa et al. (1993), with synthetic seismograms computed by the modal summation technique (Panza, 1985; Panza and Suhadolc, 1987; Florsch et al., 1991). Only receivers inside Greece are taken into account. We estimate the maximum ground acceleration, velocity and displacement (AMAX, VMAX and DMAX) for frequencies up to 1 Hz. Although the synthetic seismograms are computed for all three components of motion, we consider only the resultant of the horizontal components and we estimate the PGA as specified at the end of Section 7.

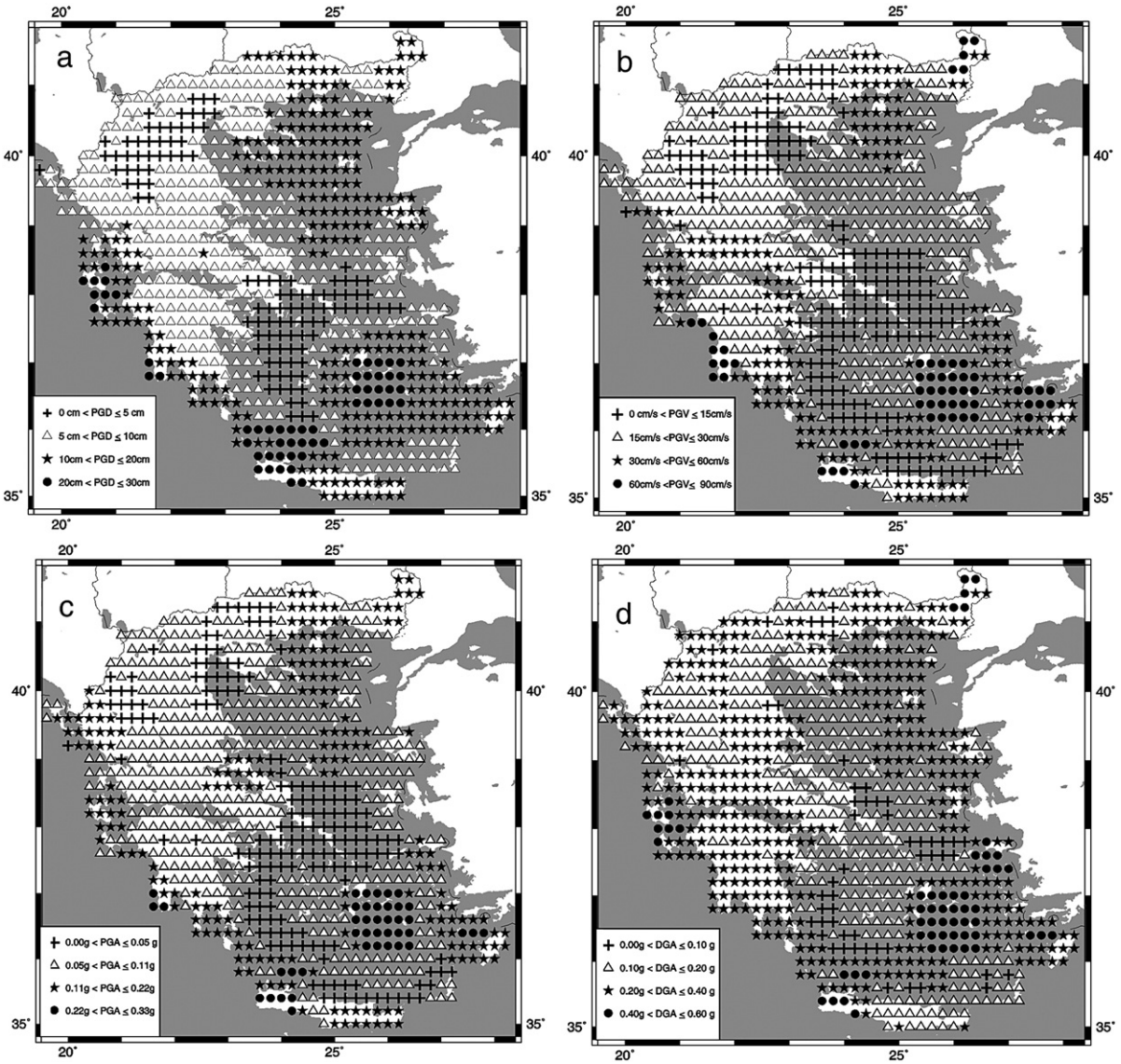

Fig. 7. Estimated maximum 1 Hz ground displacements (9a, in cm), 1 Hz velocities (9b, in cm/s), 1 Hz accelerations (9c, in *g*) and design ground accelerations (9d, in *g*) in Greece.

In Fig. 7a the maximum 1 Hz (spectral) ground displacement is plotted. The highest values (black circles) are found in the western Crete Island and near the Cephalonia fault, at the Ionian Islands (Cephalonia, Zakynthos and Lefkas), where the ground displacement can reach up to 30 cm. Another area with high values is placed in the SW Peloponnesus and in the central Aegean area. Black stars (ground displacements up to 20 cm) are placed in the western Peloponnesus, in the northern Aegean Sea and near the eastern border with Turkey (the town of Alexandroupolis). The maximum 1 Hz spectral ground displacement is less than 10 cm in all other zones. The maximum 1 Hz (spectral) ground velocity values (Fig. 7b) can reach values up to 90 cm/s at the western Crete Island, in the western Peloponnesus, in the central Aegean Sea and in some areas near the eastern border with Turkey. High values (black stars, where the ground velocity can reach 60 cm/s) are placed also in other zones of Peloponnesus, in the Ionian Islands and in some areas of Aegean Sea and eastern Greece. Fig. 7c shows the results for the geographical distribution of the maximum 1 Hz (spectral) ground accelerations. The most dangerous zones are again the western Crete Island and the central Aegean Sea (accelerations at 1 Hz can be as high as 0.33 *g*). High 1 Hz acceleration values can also be seen in the areas of Ionian Islands, Rhodes Island and in Thrace and Epirus (accelerations up to 0.22 *g*). In case of the DGA (Fig. 7d) the values are very high in western Crete Island, in the Ionian Islands (Cephalonia, Zakynthos and Lefkas), in central Aegean Sea, in Thrace and at the Samos and Rhodes Islands (the DGA values can reach 0.60 g). There are also black stars in the areas Peloponnesus and Thessalia and in all eastern Greece (the DGA values can reach 0.40 *g*).

Comparing the final results (Fig. 7) with the smoothed distribution of magnitude (Fig. 6), one can observe that high magnitude values are placed near Crete, in the Ionian Islands (Cephalonia, Zakynthos and Lefkas), in Thrace and in some areas of the Aegean Sea. The computed ground motion maps nicely reflect this, indicating the expected degree of shaking these zones could experience. These zones have therefore the most severe hazard due to shallow earthquakes of all the Aegean area. These results are clearly heavily dependent of the chosen earthquake catalogue with its spatial distribution of magnitudes. Of course our results for the Western part of Crete Island have been influenced very much by the 365 AD earthquake (M=8.3). Another important event, the 1752 AD (M=7.5) at Thrace (NE Greece), produces high values of ground motion, even though this area is characterized by low seismic hazard, when we look at maps computed with other approaches and belongs to the Zone I (lowest hazard) of the Greek seismic code. At the same time a severe hazard level is computed near Rhodes and Cephalonia Islands due to the strong seismic events clusters in the same zones. These differences arise from the fact that our maps reflect the maximum estimated ground motion parameter irrespective of the probability of its occurrence.

9. Comparison with observed data

The only way to validate our results is to compare them with the available historical and instrumental information. The only available information that spans such a long time period is the observed macroseismic intensity. We therefore compare the computed DGA with PGA estimated from the conversion of macroseismic intensity (I_{MM} to PGA, PGV and PGD) using the Theodulidis and Papazachos (1992) relations:

$$\ln a_g = 0.40 + 0.67 I_{MM} + 0.61 P \quad (1)$$

$$\ln v_g = -3.02 + 0.79 I_{MM} + 0.70 P \quad (2)$$

$$\ln d_g = -5.92 + 0.96 I_{MM} + 1.26 P \quad (3)$$

The calculations are performed for a grid of points equally spaced at 0.1°×0.1°, covering the area bounded between 34°N–42°N and 19°E–30°E. For every point the maximum intensity was selected between observed (Papazachos et al., 1997, 1999b, 2001) or theoretically estimated based on the methodology proposed by

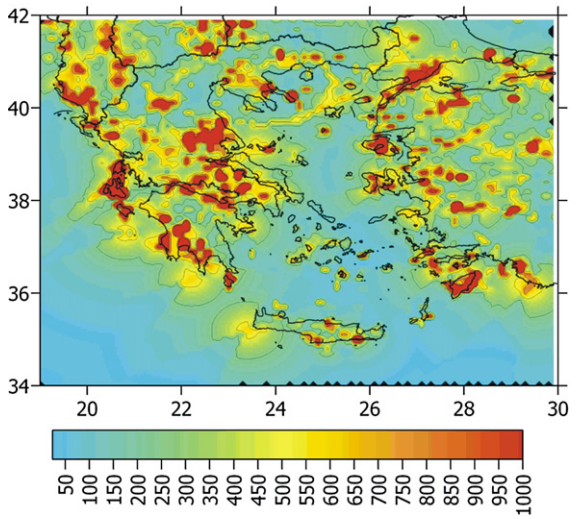

Fig. 8. Geographical distribution of the PGA (in cm/s^2) using the mean+1 sigma relation (1) for the conversion derived from observed macroseismic intensity.

Papazachos (1992). The data covers the period 426 BC–2003. The results shown in the map of Fig. 8 were compiled in terms of the SURFER ver 7.0 program using the "Inverse Distance to the Power of 2" method and search radius 0.1. There is therefore no smoothing and accelerations higher than 1 g are not shown in the map. The difference between the two maps shown is related to the scaling relation used for the conversion. The map (Fig. 8) is compiled using the mean+1 sigma. Deterministic results (Fig. 7d for DGA values) are very similar to acceleration estimated with Eq. (1) in large areas, except for the Ionian and Rhodes Island where the macroseismic intensity converts to higher ground motion values. The comparison between Fig. 7d (referred to our DGA estimation) and Fig. 8 (referred to mean+1 sigma macroseismic intensity estimation) shows that the areas with severe hazard are very similar (Ionian Islands, Rhodes, SW Peloponnesus and Thessalia). The results are, however, different in Crete and Thrace, where it seems that macroseismic intensities due to historical earthquakes (M=8.3 in 365 AD near Crete; M=7.5 in 1752 AD in Thrace) were limited and moreover smoothed during the contouring procedure. In general these maps result in higher values (on average twice) than those of DSHA results, because intensity is very sensitive to local site effects that amplify waves and produces more damages, whereas the modal summation technique estimates ground motion for bedrock conditions.

10. Estimation of influence of the velocity model and source finiteness on the final results

We test different proposed velocity models for a given seismogenic area to estimate the influence of the velocity model on our results. We select a few different velocity models for the regional polygons (see Fig. 4) number 1 (Peloponnesus) and number 5 (Crete Island). In the models used previously there was a low-velocity crustal layer (Karagianni et al., 2002, 2005), whereas the two models proposed by Papazachos et al. (1995) and Papazachos and Nolet (1997) do not have any channel in the crust. The models used to obtain the results of Fig. 5 are called "kar001" and "kar005", the alternative models, plotted in Fig. 9, are called "pap001" and "pap005".

In Polygon 1 the "kar001" and "pap001" models have the same parameters for the mantle structure. At the surface "kar001" has slower layers (Vs=1.80 km/s) than "pap001", the latter being faster also in the lower crust. The "kar001" model has a fast layer (Vs=3.40 km/s) in the 2–7 km depth range, but the greatest difference is noticed in the 7–15 km depth range: in "kar001" there is a low-velocity zone (Vs=3.20 km/s), whereas "pap001" has no crustal channel. In polygon 5 the models called "kar005" and "pap005" have the same parameters for the surface layers and the same for the mantle structure. In the crust the model "kar005" has faster layers than "pap005". A low-velocity crustal zone is also placed in the 6–11 km depth range in the "kar005" model.

After computing the synthetic seismograms and extracting the peak ground motion parameters, we have calculated the differences between the values obtained using the "kar001" and "kar005" models and those computed using "pap001" and "pap005" models. To analyze the results, we use relative differences defined as the ratio between the difference value and the related average value (Taylor, 1986). The difference and the average value are computed for each receiver and the relative and the percentual difference are obtained. The relative differences have been plotted in Fig. 10 where the data are divided into five ranges: ((−0.8)–(−0.4) crosses), ((−0.4)–0.0 triangles), (0.0–0.4 squares), (0.4–0.8 circles) and (0.8–

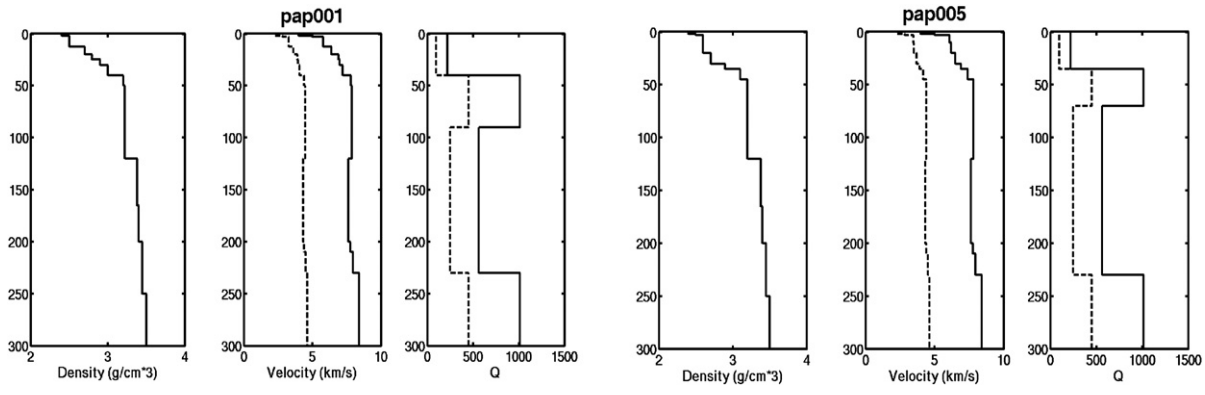

Fig. 9. Lithospheric velocity models as a function of depth (solid lines show P-wave data, dotted lines show S-wave data) for the models "pap001" (top) and "pap005" (bottom).

1.2 squares). Generally the maximum ground motion values computed with model "kar001" are higher in polygon 1, whereas the model "pap005" produces the highest values in polygon 5. In polygon 5 the absolute percentual differences are less than 40% for velocity, acceleration and design ground acceleration, but they are higher for the displacement. In Northern Crete Island the model "kar005" gives the strongest maximum ground motion, whereas "pap005" gives the highest values in Southern Crete Island. In Peloponnesus the absolute percentual differences are less than 40% for velocity, acceleration and design ground acceleration. Also in this case we obtain the highest differences for the displacement case, the values being high in Southern Peloponnesus and in the Ionian Islands where the relative differences can reach 0.8. However, the values are mainly in the range (−0.4, +0.4) for the land receivers and these results essentially do not depend on the type of ground motion (displacement, velocity, acceleration…). Of course the majority of high values (crosses, circles and squares) are placed at sea, where we do not consider seismic hazard.

In our subsequent analysis we extract the mean value (ε) and the standard deviation (σ) for the relative differences applying the definition proposed by Taylor (1986). The mean values are again computed separately for the Polygons 1 and 5 to test the different structural effects in the different Aegean areas. All sites (placed on land or at sea) have been used to have a large number of receivers and a good estimate of the mean value. The results are reported in Table 3: the mean values are very similar for the different ground motion components in the same structural polygon. But there is a large difference in the mean value between the Peloponnesus zone (higher positive values) and the Crete Island zone (lower negative values). We can state that in Polygon 1 there is an important difference in changing the structural model while this difference is not important for what concerns Polygon 5. Generally standard deviations are lower for displacement and higher for acceleration and DGA. We analyzed more closely the relative differences as a function of the source–receiver distance and as a function of the azimuth between the source fault plane strike and the direction of the ray between the source and the receiver. The azimuthal angle between the strike line and the line joining the source and the receiver has been measured counterclockwise from the right hand side of the strike line as one stands on the footwall facing the strike line. The distributions of relative differences are a function of the distances between the source and the receiver and indicate that no dependence can be observed

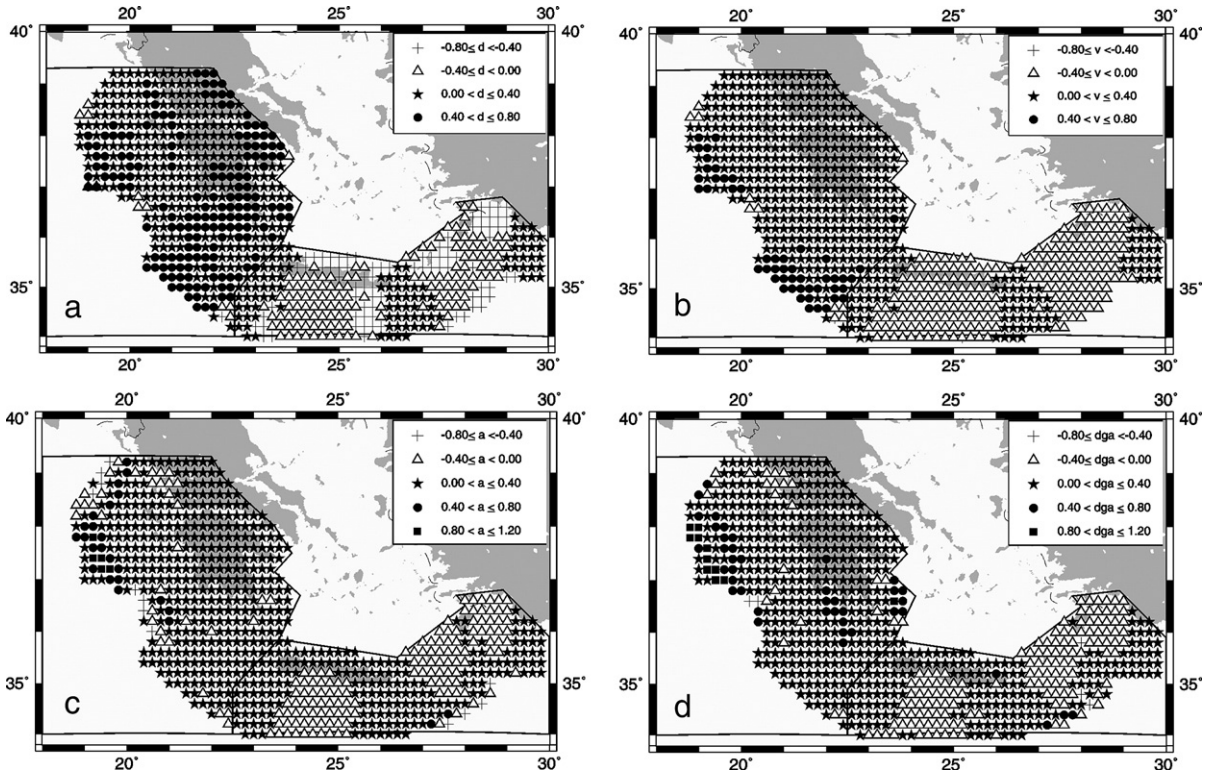

Fig. 10. Relative differences for displacements (12a), velocities (12b), acceleration (12c) and DGA (12d) along the Hellenic trench.

Table 3
Mean values and standard deviations (Taylor, 1986) of the ground motion relative differences for Polygon 1 (424 receivers) and Polygon 5 (316 receivers)

Ground motion	ε (1)	σ (1)	ε (5)	σ (5)
PGD	0.2420	0.1226	−0.0579	0.0883
PGV	0.2265	0.1582	−0.0147	0.0945
PGA	0.1690	0.2012	−0.0099	0.1248
DGA	0.2530	0.2188	−0.0148	0.1412

in Peloponnesus area, while the relative differences are quite sensitive to distances greater than 50 km in Crete Island (there are only negative values): of course the relative differences increase when the source–receiver distance is greater than 50 km because of the influence of the crustal channel on the signals. Polygon 1 presents higher values because of the differences in the surface layers of the two models. There is no evident relation between the azimuthal angles and the relative differences and no conclusions can be reached in this case. Furthermore, the relative differences do not depend on the magnitude distribution, contrary to the maximum ground motion amplitudes.

We evaluate the different influence of velocity models on the final hazard testing two different structural models without the presence of slow surface layers and the channel in the Peloponnesus area. The first new model "kar001s" is obtained changing the surface layers (from 1.8 km/s to 3.4 km/s for the S-wave velocity); the second model "kar001c" is exactly the same as the original "kar001", but we eliminate the low-velocity channel in the 7–15 km depth range. The PGV values are computed with the deterministic method for all receivers placed in the area of structural model 1; in both cases we computed the ratio between the new PGV estimations and the related values obtained previously with velocity model "kar001". The mean values are, respectively, 0.86 (std = 0.07) using model "kar001c" (no channel presence) and 0.59 (std = 0.31) using model "kar001s" (no slow surface layers). There is no evident correlation between the ratio and the magnitude distribution or the source–receiver azimuth. More interesting is the PGV ratio as a function of the epicentral distance (Fig. 11): when model "kar001c" is used the ratio is greater than 0.8 and stable within a distance of 50 km, even if the scattering effect increases for larger distances. We can deduce that the crustal channel presence influences the maximum amplitudes only for epicentral distances greater than 50 km, when the seismic rays are affected by the low-velocity layers; very often however the most important results for the hazard are obtained for areas near the seismic source. On the contrary, surface layers (model "kar001s") influence in a very strong way the ground motion amplitude and the scattering is quite large for all epicentral distances. Although surface layers are very important in estimating seismic hazard, our models do not take into account local site effects because compute ground motion for bedrock conditions. Once we extract the engineering parameters (PGD, PGV, PGA and DGA) from the synthetic seismograms computed for bedrock, we could add some site-amplification factor related to receiver, but this would require a punctual knowledge of the local geology at all receivers. Anyway, a possible future development of this modeling could be the rough use of the three simplified soils definition given in EC8 and computing site-specific DGA values. The deterministic modeling allows us to estimate the strongest hazard over a much extended area (e.g. Italy, India, Greece…) but a modified methodology must be adopted for considering the specific characteristics of each seismic source and receiver (Suhadolc et al., 2007).

The influence of the extended source is evaluated performing a test in the Kozani area. We compute

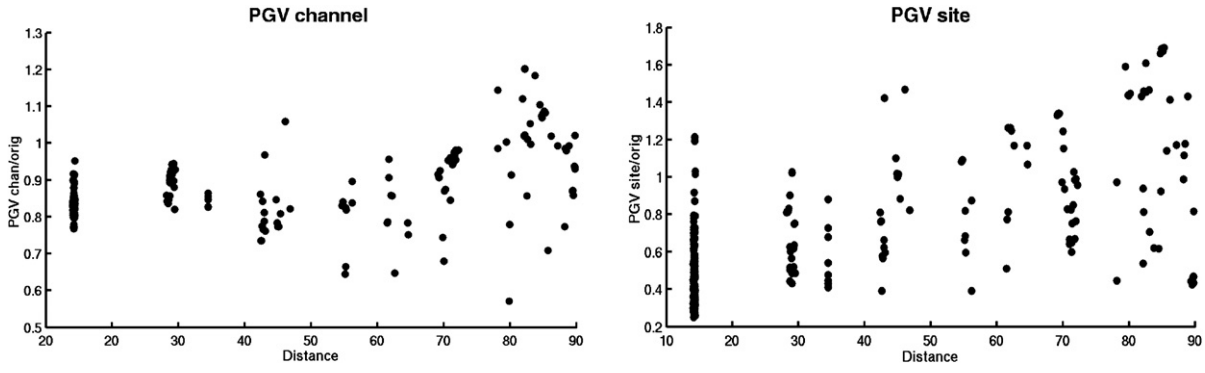

Fig. 11. PGV ratio as a function of epicentral distance for velocity models "kar001c" (on the left) and "kar001s" (on the right) with respect to the original model "kar001".

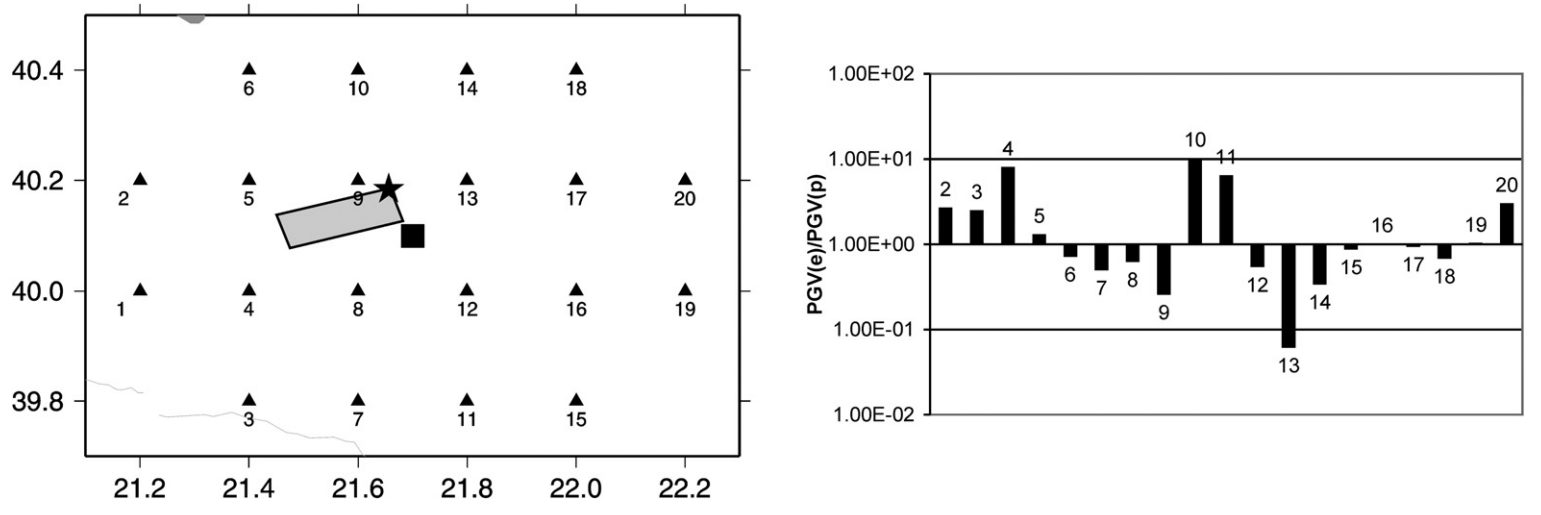

Fig. 12. Above the map for the Kozani scenario: the triangles are the receivers, the square is the epicenter placed on the center of the cell by the deterministic model, the star is the nucleation of the extended fault (grey rectangle). Below the histograms of the PGV ratio for each receiver; site 1 is missing because it is too large for the figure.

synthetic seismograms near the source applying two different models, the scaled point-source deterministic approach (Costa et al., 1993) and the extended source model. In this second case we select the needed source parameters and compute the signals following Suhadolc et al. (2007), the PGV values being computed at the same receivers used for the deterministic model (Fig. 12a). The ratio of the two PGV is computed for each site and it is plotted as histograms (Fig. 12b). The epicenter position is slightly different in the two models because in the deterministic approach the source is placed the source at the center of the cell. Also the presence of a finite rupture area might be important, because the distance between the source and the receiver (and thus the PGV value) changes considerably. However in the deterministic modeling the application of the smoothing window allows us to enlarge the source area and thus to resolve this problem. The strongest ratio, a value of about 150, is computed for site 1, because the directivity effect (Archuleta and Hartzell, 1981) produces very high PGV values in the forward directivity region, while the point-source model cannot reproduce this effect. Large differences in PGV, due to the directivity, are observed also at sites 4 and 13; the directivity influences very much the final results, but it is the most difficult parameter to estimate in a simple deterministic hazard because the same fault could nucleate at different positions on the fault leading to rupture propagating in different/opposite directions. On the other side our point-source model takes into account some effects of the finite fault, because the computed synthetic seismograms are scaled in frequency to the proper seismic moment value applying empirical Gusev curves (1983) similar to the ω^2-squared source model.

11. Conclusions

The maximum ground motion is estimated for shallow earthquakes in Greece applying the deterministic seismic hazard analysis (DSHA) of Costa et al. (1993). Available data about magnitude distribution, seismic sources, structural models and seismogenic zones are used to estimate the hazard. The Papazachos and Papazachou (2003) seismicity catalogue for the Aegean area is used and 67 different seismogenic zones defined. In each seismogenic zone a representative focal mechanism is fixed and a velocity model (eight in total) selected for every regional structural area. The maximum ground motion amplitudes are computed for 1 Hz displacement, velocity and acceleration and for the design ground acceleration, applying the modal summation technique to compute synthetic seismograms (Panza, 1985; Panza and Suhadolc, 1987; Florsch et al., 1991). The results show that the most severe hazard is located in the SW Peloponnesus, in the Ionian Islands (Cephalonia, Zakynthos and Levkas), in the Crete and Rhodes Islands and in eastern Greece.

The highest obtained values of the ground motion parameters were found in the central Aegean Sea, in the Ionian Islands (Cephalonia, Zakynthos and Lefkas), in the Rhodes and Crete Islands and in eastern Greece. The magnitude distribution (Fig. 6) is crucial to estimate the DSHA since the strongest event(s) in the area control(s) the final results: of course our results for the Western part of Crete Island has been influenced very much by the 365 AD earthquake (M=8.3). Similarly the 1752 AD event (M=7.5) at Thrace (NE Greece) produces high values of ground motion, even though this area is characterized by low seismic hazard when we look at maps computed with other approaches and belongs to the Zone I (lowest hazard) of the Greek seismic code. It is important to notice that a crude oil pipeline is going to be constructed in this area. At the same time a severe hazard level is estimated near Rhodes and Cephalonia Islands due to the strong seismic events clusters in the same zones. Qualitatively, these observations are in agreement with the compiled seismic hazard maps but the latter values are much higher. Since the DSHA hazard controls the results of the strongest earthquake occurred in the selected area, the deterministic prediction is strongly influenced by the errors in location and magnitude of strong earthquakes, particularly for historical events. The smoothing procedure of magnitudes applied in DSHA only partly overcomes the influence of such errors.

Different velocity models for the same seismogenic area are tested to study the influence of a particular velocity model on the final results of the DSHA. These tests demonstrate that the surface layers influence very much the final results, while the presence of the crustal channel is less sensitive within epicentral distance of 50 km. Therefore, the selection of a velocity models is of fundamental importance when applying the deterministic approach, as already observed in previous studies (Suhadolc and Chiaruttini, 1987; Douglas et al., 2004).

The influence of the finiteness of the fault for large events has been tested for the Kozani earthquake case by estimating PGV with two approaches: the DSHA one with scaled point-source and the finite-source modeling proposed by Suhadolc et al. (2007). Strong differences on the final results are mainly due to the well-known directivity effect and this is certainly a limitation in the Costa et al. (1993) DSHA approach. On the other side the application of a smoothing window reduces the influence of the source spatial extent.

The scaled point-source model is not the only approximation used in this study. The synthetic seismograms are computed with a 1-D velocity model (at the receiver), whereas laterally heterogeneous models (if known) should in principle produce better results. Finally, we are taking into account site effects and our results are valid only for bedrock conditions. Again, a detailed modeling is appropriate in the presence of a known laterally heterogeneous subsurface structure, but simple first-order estimates are also possible when site effect amplifications have been empirically or theoretically studied for specific sites (Suhadolc et al., 2007).

Acknowledgments

This work was performed in the framework of the EU contract EVG1-CT2001-00040: EUROSEISRISK — Seismic Hazard Assessment, Site Effects and Soil Structure Interaction in an Instrumented Basin. This work began when one of the authors, B.O.S., benefited from Marie-Curie Training site contract in Trieste (EVK2-CT-2000-57002).

References

Algermissen, S.T., Perkins, D.M., Isherwood, W., Gordon, D., Reagor, G., Howard, C., 1975. Seismic risk evaluation of the Balkan region. Proc. Sem.: Seismic Zoning Maps, Skopje, vol. 2, pp. 172–240.

Ambraseys, N.N., Douglas, J., Sarma, S.K., Smit, P.M., 2005. Equations for the estimations of strong ground motions from shallow crustal earthquakes using data from Europe and the Middle East: horizontal peak ground acceleration and spectral acceleration. Bull. Earthqu. Eng. 3, 1–53.

Aoudia, K., Vaccari, F., Suhadolc, P., Meghraoui, M., 2000. Seismogenic potential and earthquake hazard assessment in the Tell Atlas of Algeria. J. Seismol. 4, 79–98.

Archuleta, R.J., Hartzell, S.H., 1981. Effect of fault finiteness on near-source ground motion. Bull. Seismol. Soc. Am. 71, 939–957.

Birch, F., 1969. Density and compositions of the upper mantle: first approximation as an olivine layer. In: Hart, P.J. (Ed.), Geophysical Monograph 13: the Earth's Crust and Upper Mantle. AGU, Washington, D.C., pp. 18–36.

Burton, P.W., Xu, Y., Tselentis, G.A., Sokosand, E., Aspinall, W., 2002. Strong ground acceleration seismic hazard in Greece and neighboring regions. Soil Dyn. Earthqu. Eng. 23, 159–181.

Bus, Z., Szeidovitz, G., Vaccari, F., 2000. Synthetic seismograms based deterministic seismic zoning of the Hungarian Part of the Pannonian Basin. Pure Appl. Geophys. 157, 205–220.

Comninakis, P.E., Papazachos, B.C., 1986. A catalogue of earthquakes in Greece and the surrounding areas for the period 1901–1985. Publ. Geophys. Lab. Univ. Thessaloniki.

Costa, G., Panza, G.F., Suhadolc, P., Vaccari, F., 1993. Zoning of the Italian territory in terms of expected peak ground acceleration derived from complete synthetic seismograms. J. Appl. Geophys. 30, 149–160.

Douglas, J., Suhadolc, P., Costa, G., 2004. On the incorporation of the effect of crustal structure into empirical strong ground motion estimation. Bull. Earthqu. Eng. 2, 75–99.

Drakopoulos, J., Makropoulos, K., 1983. Seismicity and Hazard Analysis Studies in the Area of Greece. Publ. Seism. Lab. Univ. of Athens, vol. 1. 126 pp.

El-Sayed, A., Vaccari, F., Panza, G.F., 2001. Deterministic seismic hazard in Egypt. Geophys. J. Int. 144, 555–567.

Florsch, N., Fah, D., Suhadolc, P., Panza, G.F., 1991. Complete synthetic seismograms for high-frequency multimode SH-waves. Pure Appl. Geophys. 136, 529–560.

Fowler, C.M.R., 1991. The Solid Earth, An Introduction to Global Seismology. Cambridge University Press. 471 pp.

Gusev, A.A., 1983. Descriptive statistical model of earthquake source radiation and its implication to an estimation of short period strong motion. Geophys. J. R. Astron. Soc. 74, 787–800.

Jackson, J., 1994. Active tectonics of the Aegean region. Annu. Rev. Earth Planet. Sci. 22, 239–271.

Karagianni, E.E., Panagiotopoulos, D.G., Panza, G.F., Suhadolc, P., Papazachos, C.B., Papazachos, B.C., Kiratzi, D., Hatzfeld, D., Makropoulos, K., Priestley, K., Yuan, A., 2002. Rayleigh wave group velocity tomography in the Aegean area. Tectonophysics 358, 187–209.

Karagianni, E.E., Papazachos, C.B., Panagiotopoulos, D.G., Suhadolc, P., Yuan, A., Panza, G.F., 2005. Shear velocity structure in the Aegean area obtained by inversion of Rayleigh waves. Geophys. J. Int. 160, 127–143.

Koutrakis, S.I, Koliopoulos, P.K., Karakaisis, G.F., Margaris, B.N., Hatzidimitriou, P.M., 2002. Seismic hazard in Greece based on different strong ground motion parameters. J. Earthqu. Eng. 6, 75–109.

Lay, T., Wallace, T.C., 1995. Modern Global Seismology. International Geophysics Series, vol. 58. Academic Press.

Margaris, V.N., 1994. Azimuthal dependence of the seismic waves and its influence on the seismic hazard assessment in the area of Greece, PhD. Thesis, Univ. Thessaloniki, 324 pp. (in Greek, with an English abstract).

Markusic, S., Suhadolc, P., Herak, M., Vaccari, F., 2000. A contribution to seismic hazard in Croatia from deterministic modelling. Pure Appl. Geophys. 157, 158–204.

McGuire, R.K., 1993. Computations of seismic hazard. Ann. Geofis. 36, 181–200.

McKenzie, D.P., 1970. Plate tectonics of the Mediterranean region. Nature 226, 239–243.

McKenzie, D.P., 1972. Active tectonics of the Mediterranean region. Geophys. J. R. Astron. Soc. 30, 109–185.

McKenzie, D.P., 1978. Active tectonics of the Alpine-Himalayan belt: the Aegean Sea and surrounding regions. Geophys. J. R. Astron. Soc. 55, 217–254.

Mueller, St., 1977. A new model of the continental crust. In: Heacock, J.G. (Ed.), The Earth's Crust: its Nature and Physical Properties, vol. 20. AGU, Washington, DC, pp. 289–317.

Novotny, O., Zahradnik, J., Tselentis, G.A., 2001. Northwestern Turkey earthquakes and the crustal waves observed in Western Greece. Bull. Seismol. Soc. Am. 91, 875–879.

Orozova-Stanishkova, I.M., Costa, G., Vaccari, F., Suhadolc, P., 1996. Estimation of 1 Hz maximum acceleration in Bulgaria for seismic risk reduction purposes. Tectonophysics 258, 263–274.

Panza, G.F., 1985. Synthetic seismograms: the Rayleigh waves modal summation. J. Geophys. 58, 125–145.

Panza, G.F., Suhadolc, P., 1987. Complete strong motion synthetics. In: Bolt, Bruce A. (Ed.), Seismic Strong Motion Synthetics. Academic Press, New York, pp. 153–204.

Panza, G.F., Prozorov, A., Suhadolc, P., 1990. Lithosphere structure and statistical properties of seismicity in Italy and surrounding regions. In: Danobeitia, J.J., Pinet, B. (Eds.), Geophysics of the Mediterranean Basin. Journal of Geodynamics, vol. 12, pp. 189–215.

Panza, G.F., Vaccari, F., Costa, G., Suhadolc, P., Fah, D., 1996. Seismic input modeling for zoning and microzoning. Earthq. Spectra 12, 529–566.

Papaioannou, Ch.A., 1984. Attenuation of seismic intensities and seismic hazard in the area of Greece, PhD. Thesis, Univ. Thessaloniki, 200 pp. (in Greek, with an English abstract).

Papaioannou, Ch.A., 1986. Seismic hazard assessment and long term earthquake prediction in Southern Balkan region. In: Vogel, A., Brandes, K. (Eds.), Proc. 2nd Int. Sem. on Earthquake Prognostics, FU Berlin, pp. 223–241.

Papaioannou, Ch.A., Papazachos, B.C., 2000. Time-independent and time-dependent seismic hazard in Greece based on seismogenic sources. Bull. Seismol. Soc. Am. 90, 22–33.

Papazachos, B.C., 1990. Seismicity of the Aegean and surrounding area. Tectonophysics 178, 287–308.

Papazachos, B.C., Comninakis, P.E., 1969. Geophysical features of the Greek island arc and the Eastern Mediterranean ridge. Proc. C. R. Seances de la Conference Reunie a Madrid, vol. 16, pp. 74–75.

Papazachos, B.C., Kiratzi, A.A., Hatzidimitriou, P.M., Papaioannou, Ch.A., Theodulidis, N.P., 1985. Regionalization of seismic hazard in Greece. Proc. 12th Reg. Sem. on Earthq. Eng. EAEE–EPPO, Halkidiki, Greece. 12 pp.

Papazachos, B.C., Papaioannou, Ch.A., Papastamatiou, D.J., Margaris, V.N., Theodulidis, N.P., 1990. On the reliability of different methods of the seismic hazard assessment in Greece. Nat. Hazards 3, 141–151.

Papazachos, B.C., Papaioannou, Ch.A., 1993. Long-term earthquake prediction in the Aegean area based on a time and magnitude predictable model. Pure Appl. Geophys. 140, 595–612.

Papazachos, B.C., Papaioannou, Ch.A., Margaris, V., Theodulidis, N., 1993. Regionalization of seismic hazard in Greece based on seismic sources. Nat. Hazards 8, 1–18.

Papazachos, B.C., Papaioannou, Ch.A., Papazachos, C.B., Savvaidis, A.S., 1997. Atlas of isoseismal maps for strong shallow earthquakes in Greece and surrounding area (426 BC–1995). Univ. of Thessaloniki, Geophys. Laboratory, 4, 1997, 176 pp.

Papazachos, B.C., Papadimitriou, E.E., Kiratzi, A.A., Papazachos, C.B., Louvari, E.K., 1998. Fault plane solutions in the Aegean Sea and the surrounding area and their tectonic implication. Boll. Geofis. Teor. Appl. 39, 199–218.

Papazachos, B.C., Papaioannou, Ch.A., Papazachos, C.B., Savvaidis, A.S., 1999a. Rupture zones in the Aegean region. Tectonophysics 308, 205–221.

Papazachos, B.C, Savaidis, A.S., Papaioannou, Ch.A., Papazachos, C.B., 1999b. The S. Balkan Bank of Shallow and Intermediate Depth Earthquake Macroseismic Data, XXII Gen. Ass. of the IUGG, Birmingham, UK July 1999. abstracts volume.

Papazachos, B.C., Papaioannou, Ch.A., Papazachos, C.B., Kiratzi, A.A., Muco, B., Kociu, S., Sulstarova, E., 2001. Atlas of isoseismal maps for strong shallow earthquakes in Albania and surrounding area (1851–1900). Univ. of Thessaloniki, Geophys. Laboratory, 10. 57 pp.

Papazachos, B.C., Papazachou, C.C., 2003. Earthquakes of Greece. Ziti Publications, Thessaloniki. 286 pp., (in Greek).

Papazachos, C.B., 1992. Anisotropic radiation modelling of macroseismic intensities for estimation of the attenuation structure of the upper crust in Greece. Pure Appl. Geophys. 138, 445–469.

Papazachos, C.B., 1999. Seismological and GPS evidence for the Aegean–Anatolia interaction. Geophys. Res. Lett. 17, 2653–2656.

Papazachos, C.B., 2002. A tecto-kinematic model for the Aegean using seismological and GPS data. Proc. 11th Gen. Ass. WEGENER, Athens, GREECE, 12-14 June, 2002. 19pp.

Papazachos, C.B., Nolet, G., 1997. P and S deep velocity structure of the Hellenic area obtained by robust nonlinear inversion of travel times. J. Geophys. Res. 102, 8349–8367.

Papazachos, C.B., Hatzidimitriou, P.M., Panagiotopoulos, D.G., Tsokas, G.N., 1995. Tomography of the crust and upper mantle in southeast Europe. J. Geophys. Res. 100, 12405–12422.

Radulian, M., Vaccari, F., Mandrescu, N., Panza, G.F., Moldoveanu, C.L., 2000. Seismic hazard of Romania: deterministic approach. Pure Appl. Geophys. 157, 221–247.

Scordilis, E.M., Karakaisis, G.F., Karakostas, E.G., Panagiotopoulos, D.G., Comninakis, P.E., Papazachos, B.C., 1985. Evidence for transform faulting in the Ionian Sea. The Cephalonia island earthquake sequence of 1983. Pure Appl. Geophys. 123, 388–397.

Suhadolc, P., 1990. Fault-plane solutions and seismicity around the EOT southern segment. In: Freeman, R., Mueller, St. (Eds.), Proc. 6th Workshop on the European Geotraverse (EOT), Data compilations and Synoptic Interpretation. European Science Foundation, Strasbourg, pp. 371–382.

Suhadolc, P., Chiaruttini, C., 1987. A theoretical study of the dependence of the peak ground acceleration on source and structure parameters. In: Erdik, M.O., Toksoz, M.O. (Eds.), Strong Ground Motion Seismology. Reidel, Dordrecht, pp. 143–183.

Suhadolc, P., Moratto, L., Costa, G., Triantafyllidis, P., 2007. Source modelling of the Kozani and Arnea events with strong motion estimates for the city of Thessaloniki. J. Earthqu. Eng. 11, 560–581.

Taylor, J.R., 1986. Introduzione all'analisi degli errori − Lo studio delle incertezze nelle misure fisiche. Zanichelli, Bologna.

Taymaz, T., Jackson, J., McKenzie, D., 1991. Active tectonics of the north central Aegean Sea. Geophys. J. Int. 106, 433–490.

Theodulidis, N., Papazachos, B.C., 1992. Dependence of strong ground motion on magnitude–distance, site geology and macroseismic intensity for shallow earthquakes in Greece: I. Peak horizontal acceleration, velocity and displacement. Soil Dyn. Earthqu. Eng. 11, 387–402.

Zahradnik, J., Papatsimpa, K., 2001. Focal mechanism of weak earthquakes from amplitude spectra and polarities. Pure Appl. Geophys. 158, 647–665.

Zivcic, M., Suhadolc, P., Vaccari, F., 2000. Seismic zonation of Slovenia based on deterministic hazard computation. Pure Appl. Geophys. 157, 171–184.